DMD Fast Forward. Published on June 23, 2017 as DOI: 10.1124/dmd.117.075929
This article has not been copyedited and formatted. The final version may differ from this version.

Title Page

Stereospecific Metabolism of *R*- and *S*-Warfarin by Human Hepatic Cytosolic Reductases

Barnette, Dustyn A., Johnson, Bryce P., Pouncey, Dakota L., Nshimiyimana, Robert.

Desrochers, Linda P., Goodwin, Thomas E., Miller, Grover P.

Department of Biochemistry and Molecular Biology, University of Arkansas for Medical Sciences, Little Rock, AR 72205, USA (DAB, DLP, GPM)

Department of Chemistry, University of Central Arkansas, Conway, AR 72035, USA (BPJ)

Department of Chemistry, Hendrix College, Conway, AR 72032, USA (RN, LPD, TEG)

Running Title Page

Stereospecific *R*- and *S*-Warfarin Reduction in the Cytosol

Address for Correspondence

Grover P. Miller, PhD

Department of Biochemistry and Molecular Biology

University of Arkansas for Medical Sciences

4301 W. Markham, Slot 516.

Little Rock, AR 72205, USA;

Telephone: 501.526.6486;

Fax: 501.686.8169;

Email: MillerGroverP@uams.edu

Number of Text Pages: 14

Number of Tables: 1

Number of Figures: 6

Number of References: 39

Number of words in the *Abstract*: 239

Number of words in the *Introduction*: 700

Number of words in the *Discussion*: 1217

Abbreviations

WAR, warfarin; WAROH, warfarin alcohol; HOWAR, hydroxywarfarin; FFA, flufenamic acid; INDO, indomethacin; QUE, quercetin; AKR, aldo-keto reductase; CBR, carbonyl reductase

Abstract

Coumadin (rac-warfarin) is the most commonly used anticoagulant in the world, yet its clinical use is often challenging due to a narrow therapeutic range and inter-individual variations in response. A critical contributor to the uncertainty is variability in warfarin metabolism, which includes mostly oxidative but also reductive pathways. Reduction of each warfarin enantiomer yields two warfarin alcohol isomers, and the corresponding four alcohols retain varying levels of anticoagulant activity. Studies on the kinetics of warfarin reduction have often lacked resolution of parent drug enantiomers and suffered from co-elution of pairs of alcohol metabolites; thus, those studies fail to establish the importance of individual, stereospecific reductive pathways. We report the first steady-state analysis of *R*- and *S*-warfarin reduction *in vitro* by pooled human liver cytosol. As determined by authentic standards, the major metabolites were 9R,11S-warfarin alcohol for *R*-warfarin, and 9S,11S-warfarin alcohol for *S*-warfarin. *R*-warfarin (V_{max} 150 pmol/mg/min, K_m 0.67 mM) was reduced more efficiently than *S*-warfarin (V_{max} 27 pmol/mg/min, K_m 1.7 mM). Based on inhibitor phenotyping, carbonyl reductase-1 dominated *R*- and *S*-warfarin reduction followed by aldo-keto reductase-1C3 and then other members of that family. Overall, the carbonyl at position 11 undergoes stereospecific reduction by multiple enzymes to form the *S* alcohol for both drug enantiomers, yet *R*-warfarin undergoes reduction preferentially. This knowledge will aid in assessing the relative importance of reductive pathways for *R*- and *S*-warfarin and factors influencing levels of pharmacologically active parent drugs and metabolites thus impacting patient dose-responses.

Introduction

Coumadin is a commonly used blood thinner worldwide that consists of a 1:1 mixture of *R*- and *S*-warfarin (Figure 1) (Ansell et al., 2008). The anticoagulant effect of warfarin reflects inhibition of VKORC, which plays a critical role in vitamin K cycling and the maturation of coagulation factors. Though very efficacious, warfarin can be difficult to optimally treat patients due to its narrow therapeutic range and inter-individual variations in response. Doses have to be individually established for each patient based on how they respond to the medication. Failure to achieve and maintain an optimal dose for patients increases risks for potentially life-threatening adverse events due to under dosing (strokes) and over dosing (bleeding) (Wysowski et al., 2007). Knowledge of the causes of this variability in dose-responses can then lead to better management strategies.

Inter-individual variations in patient dose-responses to warfarin often reflect the importance of drug metabolism(Jones and Miller, 2011). Cytochromes P450 oxidize *R*- and *S*-warfarin into hydroxywarfarins, and as major routes for drug clearance, those metabolic pathways have dominated the focus of most studies. Through minor, less characterized pathways, both drugs also undergo reduction at the carbonyl at position 11 to yield warfarin alcohols. Warfarin reduction introduces a second chiral center, making two of warfarin alcohol diastereomers for each warfarin enantiomer. For R-warfarin, the two metabolites are *9R,11R*- or *9R,11S*-warfarin alcohol (*RR*- or *RS*-warfarin alcohol), and for *S*-warfarin, they are *9S,11S*- and *9S,11R*- warfarin alcohol (*SS*- or *SR*-warfarin alcohol). Warfarin alcohols retain pharmacological activity that is 6-fold lower than that for the parent drugs (Gebauer, 2007); however, clearance of *RS*-warfarin alcohol is 2.5-fold lower than the other alcohols indicating selective accumulation of the metabolite in plasma based on stereochemistry (Lewis, 1973), which increases their relative potency during maintenance dosing (Haque et al., 2014). According to a previous report (Haque et al., 2014), warfarin alcohols are the most potent of the warfarin metabolites,

DMD Fast Forward. Published on June 23, 2017 as DOI: 10.1124/dmd.117.075929
This article has not been copyedited and formatted. The final version may differ from this version.

contributing 15% of the anticoagulant effect of S-warfarin for the average patient at a maintenance dosing. Consequently, knowledge of the impact of stereochemistry on *R*- and *S*-warfarin reduction is critical for adequately assessing the clinical relevance of those pathways.

Recent studies using subcellular fractions from rats (Alshogran et al., 2015a) and humans (Malátková et al., 2016) have provided limited insights on reductive pathways for warfarin due to reliance on rac-warfarin and not the actual drug enantiomers as a substrate and the subsequent lack of chiral resolution of metabolites from the reaction. First, the drug is administered as a 1:1 mixture of enantiomers, but those conditions do not reflect patient serum levels and mask actual clearance of individual warfarin enantiomers. Reported *R*-warfarin levels in patients are on average two-fold higher than *S*-warfarin(Breckenridge et al., 1974; Jones et al., 2010; Haque et al., 2014). Knowledge of the metabolic kinetics for individual drug enantiomers would provide perspective for assessing their relative significance in drug clearance. Moreover, the use of a mixture of substrates in those studies masks possible drug-drug interactions between the enantiomers, which were implicated in one of the studies(Malátková et al., 2016). Second, it is not possible to extrapolate the metabolic kinetics for *R*- and *S*-warfarin from those for rac-warfarin so that knowledge of the impact of stereochemistry on metabolic clearance of the drugs remains unknown. Third, current studies on warfarin reduction failed to resolve all four diastereomers generated during rac-warfarin reduction. Instead, reported kinetic parameters reflect the formation of mixtures of metabolites, i.e. alcohol 1 (RR- and SS-warfarin alcohols) and alcohol 2 (RS- and SR-warfarin alcohols), generated during rac-warfarin metabolism, and hence provide no information on the kinetics for individual pathways leading to specific metabolites. Taken together, the current findings provide only a qualitative perspective on warfarin reduction and lack specific quantitative details on the individual pathways that would determine their potential clinical relevance.

Herein, we report the impact of stereochemistry on the efficiency of rac-, *R*-, and *S*- warfarin reduction by pooled human liver cytosolic (HLC150) cell fractions. Due to the lack of commercially available standards, we synthesized and purified all four diastereomeric warfarin alcohols using green chemistry techniques. We then optimized reaction conditions to achieve steady state conditions and carried out kinetic studies with *R*- and *S*-warfarin along with rac-warfarin for comparison to findings from other studies. We assessed potential interactions between the drug enantiomers by simulating rac-warfarin metabolism using parameters for the individual drugs and compared them to those measured for rac-warfarin in our study and kinetic values reported in the literature that used a limited pool of cytosol fraction from five cadavers (Malátková et al., 2016). Lastly, we employed inhibitor phenotyping to identify possible reductases responsible for warfarin metabolism in cytosolic fractions.

Materials and Methods

Materials. HPLC grade methanol, acetic acid, dimethyl sulfoxide (DMSO), and NADPH were purchased from Thermo Fisher (Pittsburgh, PA) and pooled human liver cytosol (HLC150) from BD Biosciences. Diethyl ether, hydrochloric acid, ethyl acetate, acetone, and acetic acid were obtained from PHARMCO-AAPER (Brookfield, CT). Sodium borohydride and DMS0-d_6 was purchased from Sigma-Aldrich (St. Louis, MO). Rac-Warfarin, warfarin alcohol mixed isomers, and hydroxywarfarins (internal standards) were obtained from Toronto Research Chemicals (Toronto, Canada). Individual *R*- and *S*-warfarin stereoisomers were prepared in a previous study(Preston Pugh et al., 2014), while the metabolites *9R,11R*-; *9R,11S*-; *9S,11R*-; and *9S,11S*-warfarin alcohols were synthesized and purified to >98% purity.

Synthesis of warfarin alcohols through green chemistry. We prepared authentic isomers of all four diastereomeric warfarin alcohols by synthesizing *R*- and *S*-warfarin and then reducing them individually followed by isolating the individual alcohols by thin layer chromatography and cycles of recrystallization. First, *R*- and *S*-warfarin were prepared with greater than 99%

enantiomeric excess using a green chemistry procedure as described by us (Preston Pugh et al., 2014) and others (Kim et al., 2006; Wong et al., 2010). Second, reduction of *R*- and *S*-warfarin to warfarin alcohols followed a literature procedure (Trager, 1970; Chan et al., 1972). The *R*- or *S*-warfarin (50 mg, 1.62 mmol) was stirred in one mL of deionized water with sodium borohydride (7 mg, 1.85 mmol) at the ambient temperature for 2 hr. Excess sodium borohydride was neutralized by addition of one mL of 0.5 M hydrochloric acid added dropwise with stirring. The mixture was filtered and washed with water. The resulting white solid was allowed to air dry. The reduction step for each warfarin enantiomer introduced a new chiral center resulting in a pair of diastereomers, i.e. *RS* and *RR* warfarin alcohols for *R*-warfarin and the *SS*- and *SR*-warfarin alcohols for *S*-warfarin. The typical yield of each pair of diastereomers was greater than 70%.

Isolation of individual alcohol diasteromers was achieved through silica gel thin layer chromatography (TLC) followed by recrystallization. For example, a diastereomer mixture of two warfarin alcohols (either *RS* and *RR*, or *SR* and *SS)* was dissolved in the smallest amount of ethyl acetate and dropped onto a Sorbtech Silica XHL TLC plate W/UV254 (glass backed, 250 μm thickness, 20 x 20 cm dimensions). A solvent mix of 197:3 diethyl ether:acetic acid was used to effect a separation. The bottom bands of each separation were the *RR*–and *SS*-warfarin alcohols, while the top bands were the *RS* and *SR*–warfarin alcohols. TLC identity of the aforementioned diastereomers was based upon the previous research by others (Supplemental Data, (Chan et al., 1972)). Each band was carefully scraped from the glass TLC plate and ethyl acetate was added to dissolve the alcohols. After stirring, the mixture was filtered over Celite and ethyl acetate was removed by rotary evaporation. The white solid was dissolved in the smallest amount of warm acetone, and then drops of warm water were added slowly until the solution remained cloudy. At this point the solution was heated again until clear and allowed to cool at the ambient temperature until crystals appeared, at which point the

solution was cooled in ice. When crystallization ceased, the supernatant liquid was removed by pipet and the solid allowed to air dry at ambient temperature.

NMR peak assignments were made with ^{1}H, ^{13}C, COSY, DEPT, HMQC, and HMBC techniques. *RR*-Warfarin alcohol: ^{1}H NMR (DMSO-d_6, 400 MHz): δ 1.21 (3H, d, J = 6.4 Hz, H-14), 2.40 (2H, m, H-12a, H-12b), 3.66 (1H, ddq, J = 6.0, 6.4, 6.4 Hz, H-13), 4.62 (1H, dd, J = 7.8, 8.2 Hz, H-11), 7.13 (1H, dd, J = 7.3, 7.3 Hz, H-4'), 7.24 (2H, dd, J = 7.3, 7.3 Hz, H-3', H-3'), 7.28 (1H, dd, J = 0.9, 8.1 Hz, H-8), 7.33 (1H, ddd, J = 0.9, 7.4, 7.8 Hz, H-6), 7.46 (2H, d, J = 7.3 Hz, H-2', H-2'), 7.56 (1H, ddd, J = 1.4, 7.4, 8.1 Hz, H-7), 7.93 (1H, dd, J = 1.4, 7.8 Hz, H-5); ^{13}C NMR (DMSO-d_6, 400 MHz): δ 23.9 (C-14), 38.5 (C-11), 41.6 (C-12), 67.2 (C-13), 110.2 (C-3), 117.4 (C-8), 117.8 (C-10), 124.1 (C-5), 125.1 (C-6), 127.2 (C-4'), 129 (C-3'), 129.3 (C-2'), 132.9 (C-7), 144.2 (C-1'), 153.8 (C-9), 162.7 (C-4), 165.1 (C-2); *RS*-Warfarin alcohol: ^{1}H NMR (DMSO-d_6, 400 MHz): δ 1.22 (3H, d, J = 6.4 Hz, H-14), 2.09 (1H, ddd, J = 4.8, 9.4, 14.0 Hz, H-12b), 2.60 (1H, ddd, J = 3.2, 11.1, 14.0 Hz, H-12a), 3.66 (1H, m, H-13), 4.67 (1H, dd, J = 4.8, 11.1 Hz, H-11), 7.12 (1H, dd, J = 7.3 Hz, H- 4'), 7.22 (2H, dd, J = 7.3, 7.8 Hz, H-3'), 7.27 (1H, d, J = 7.9 Hz, H-8), 7.32 (1H, dd, J = 7.9, 8.0 Hz, H-6), 7.39 (2H, d, J = 7.8 Hz, H-2'), 7.55 (1H, ddd, J = 1.4, 7.9, 7.9 Hz, H-7), 7.95 (1H, dd, J = 1.4, 8.0 Hz, H-5); ^{13}C NMR (DMSO-d_6, 400 MHz): δ 24.1 (C-14), 38.3 (C-11), 41 (C-12), 67.1 (C-13), 108.7 (C-3), 117.3 (C-8), 118 (C-10), 124.4 (C-5), 125.1 (C-6), 127 (C-4'), 128.9 (C-3'), 129 (C-2'), 132.9 (C-7), 144.7 (C-1'), 154 (C-9), 164 (C-4), 164.9 (C-2).

Identification of initial rate conditions for warfarin reduction. Prior to steady-state studies, control experiments with HLC150 were carried out to determine optimal co-solvents, reaction buffers, reaction time, and protein concentration to ensure steady-state conditions and avoid confounding effects from experimental reagents. Warfarin stocks were prepared in methanol solutions to minimize co-solvent effects on reductase activity, as shown in our control experiments (see Results). Individual warfarin reactions were prepared out with 0.25 mg/mL pooled human liver cytosol (HLC150) from 150 donors, and initiated upon addition of 1 mM

NADPH (final). Reactions were incubated at 37°C with 350 rpm rotation. After 30 min, reactions were quenched with an equal volume of acetonitrile containing, 1 μM rac-8-hydroxywarfarin (final), an internal standard, which did not co-elute with warfarin or the warfarin alcohols. Quenched reactions were centrifuged at 5°C at 2500 rpm for 15 min, and the supernatant was removed for analysis by HPLC. Unless otherwise stated, all control reactions were carried out using rac-warfarin and experimental effects monitored by measuring total product formation by combining areas of alcohols 1 and 2 to take all four alcohol diastereomers into account. All control reactions were carried out in duplicate.

Analysis of warfarin reduction by HPLC. The resolution and quantitation of individual drugs and metabolites was achieved through high performance liquid chromatography (HPLC). Samples were injected onto a Waters HPLC Breeze system equipped with a 4.6 x 150 mm Zorbax Eclipse 3.5 μM XDB-C18 column (Agilent) heated to 45°C and analytes were resolved over 13 min using a gradient method with 25 mM 4-(2-hydroxyethyl)-1-piperazineethanesulfonic acid (HEPES) /NaOH solution pH 6.80 and 25:75 acetonitrile:methanol and monitored by fluorescence (excitation: 325 nm; emission: 393 nm). Peak areas were normalized to the internal standard and then quantitated relative to known standards. Reaction rates were reported as total product formed per reaction time per amount of protein (pmoles/min/mg protein).

Steady state kinetics for R-, and S-, and rac-warfarin reduction. After optimizing reaction conditions, we determined reaction kinetics for *R*-, and *S*-, and rac-warfarin. Substrate concentrations were 1000, 500, 250, 200, 125, 100, 50, and 25 μM initially. *S*-Warfarin reactions contained an additional reaction with 750 μM substrate. Reactions were performed in at least triplicate for each substrate concentration. Reaction products were separated and analyzed by HPLC and fluorescence detection as described previously. Alcohol peaks 1 and 2 or individual alcohol diastereomers were quantitated and assessed individually. Warfarin alcohol formation

DMD Fast Forward. Published on June 23, 2017 as DOI: 10.1124/dmd.117.075929
This article has not been copyedited and formatted. The final version may differ from this version.

rates were plotted as a function of substrate concentration and analyzed by comparing the fit of the data to the Michaelis-Menten equation (hyperbolic curve) and Hill equation (non-hyperbolic curve) using in GraphPad Prism (San Diego, CA). The best fit was determined using extra sum-of-squares F test.

Inhibitor phenotyping of R- and S-warfarin reduction. HLC150 phenotyping reactions were carried out using the steady state conditions established in the control experiments (see Results). We prepared all inhibitor stocks in methanol and assessed their effects against a control reaction containing just methanol at the same final percent (5% methanol). *R*- or *S*-Warfarin concentrations at 50 and 500 μM were used in the presence of three different inhibitors to selectively inhibit individual and classes of cytosolic reductases (as reviewed in (Malátková and Wsól, 2014)). Moreover, with broadly specific inhibitors, we employed concentrations about 5-fold above the reported IC_{50} to ensure target inhibition while minimizing off target effects. We used 2 μM flufenamic acid (FFA), which inhibits all Aldo-keto Reductase family 1C members (AKR1C). This concentration has also been shown to inhibit AKR1B10 activity (Zhang et al., 2013); however, levels are typically too low to be relevant for our studies, and induction was observed only in liver cancer (Laffin and Petrash, 2012). For indomethacin (IND), a high concentration (180 μM) would similarly inhibit all AKR1C members and Carbonyl Reductase 1 (CBR1), while a lower concentration (5 μM) has a more selective effect on AKR1C3 with only limited CBR1 inhibition expected. We targeted Carbonyl Reductase 1 (CBR1) activity for inhibition using 60 μM quercetin. In addition, we combined inhibitors to assess the collective contributions of AKR1C and CBR1 enzymes. AKR1B1 is also inhibited by indomethacin and quercetin (Byrns and Penning, 2009), but this enzyme is only expressed at minimal levels in the liver, except in cases of alcoholic liver disease (O'CONNOR et al., 1999). Thus, we do not expect it to significantly contribute to metabolism in our study.

Results

DMD Fast Forward. Published on June 23, 2017 as DOI: 10.1124/dmd.117.075929
This article has not been copyedited and formatted. The final version may differ from this version.

HLC150 steady state kinetics for R-, S-, and rac-warfarin reduction. Initially, we carried out control experiments to identify optimal conditions for steady-state studies as shown in Figure 2**.** Warfarin reduction was more efficient in potassium phosphate over Tris-HCl buffer, and $MgCl_2$ had no impact on reaction rates (Panel A). Variations in methanol co-solvent levels had no effect on activity while higher DMSO levels inhibited the reaction (Panel B). Observed warfarin alcohol levels increased essentially linearly with total protein concentration (Panel C). Over the course of 60 min, product formation levels were essentially linear (Panel D). Based on these studies, the standard conditions for a 30 min reaction with 0.25 mg/mL protein was 50 mM potassium phosphate 7.4, no $MgCl_2$, and 1% methanol as a co-solvent.

Stereospecificity played a significant role in the steady state reduction of warfarin enantiomers and corresponding products from cytosolic reactions (Figure 3, Table 1). The *R*-warfarin reactions yielded *RS*-warfarin alcohol as the major metabolite and *RR*-warfarin alcohol as the minor one. Both reactions were best fit to a simple Michaelis-Menten kinetic model as compared to a non-hyperbolic curve described by the Hill equation. The metabolic efficiency for formation of the *RS*-warfarin alcohol was nearly 200-fold compared to the *RR*-warfarin alcohol due almost exclusively the difference in rate of the reaction. Similarly, the reduction of *S*-warfarin yielded the analogous metabolites, i.e. *SS*-warfarin alcohol and *SR*-warfarin alcohol. The kinetic profile for *SS*-warfarin alcohol was fit to the Michaelis-Menten model, yet the predicted K_m was greater than the highest substrate concentration used in this study (1000 μM) due to solubility limits. Thus, there is more error in the kinetic constants than predicted by a fit, hence the exclusion of standard error from the Table. The *SR*-warfarin alcohol was consistently measurable but remained at the limit of quantitation so that it was not possible to determine the kinetics for its formation. Taken together, the rate of *S*-warfarin conversion to *SS*-warfarin alcohol was about 9-fold lower than that for *R*-warfarin to *RS*-warfarin alcohol at 1000 μM,

indicating a strong preference for *R*-warfarin reduction and formation of *S* alcohols regardless of substrate chirality.

In addition, we followed the experimental design reported by others(Alshogran et al., 2015a; Malátková et al., 2016) to carry out steady-state studies with rac-warfarin for comparative purposes. Unlike the previous experiments in this study, substrate concentration reflected an initial 1:1 mixture of *R*- and *S*-warfarin, and the corresponding diasteromeric metabolites were not resolved completely. We used the previously reported nomenclature(Alshogran et al., 2015a; Malátková et al., 2016) labeling the mixture of *RS*/*SR*-warfarin alcohols as warfarin alcohol 2 and the mixture of *RR*/*SS*-warfarin alcohols as warfarin alcohol 1. Both sets of data were fit to the Michaelis-Menten model indicating the eight-fold difference in efficiency for the alcohol 2 reaction was due mainly to V_{max} and not K_m for this mixed metabolite assessment of activity (Figure 4, Panel C; Table 1). The lack of resolution of the substrates or metabolites with this approach made it impossible to identify the actual major and minor metabolites for *R*- and *S*-warfarin without relying on our initial enantiospecific steady-state kinetic studies.

Inhibitor phenotyping of cytosolic enzymes responsible for R- and S- warfarin reduction. General and relatively specific reductase inhibitors indicated multiple enzymes likely contribute to overall reduction of *R*- and *S*-warfarin in the cytosol. The overall patterns of inhibition were similar between the formation of the corresponding major metabolites *RS*-warfarin alcohol and *SS*-warfarin alcohol (Figure 5). The minor metabolites *RR*-warfarin alcohol and *SR*-warfarin alcohol were measured at levels too low for quantitative kinetics. Substrate concentrations had little effect on the patterns of inhibition for the compounds with two exceptions. First, the effect of quercetin inhibition was consistently significant but reduced for S-warfarin under low substrate conditions. Second, inhibition by low indomethacin concentration (5 μM) was reduced at lower concentration for both warfarin enantiomers. By 180 μM indomethacin, all reduction rates were decreased greater than 10-fold. These findings suggest a dominant role for AKR1C3

in the reactions and possible contributions from other AKR1C members and CBR1. Quercetin mainly inhibits CBR1, and when present, reduction rates decreased by around 70-85% for *RS*- and *SS*-warfarin alcohols. Addition of 5 μM indomethacin to the quercetin reaction did not significantly impact the observed reduction rates; however by180 μM indomethacin there was a further approximate 10% decrease in rates. Unlike indomethacin, flufenamic acid had little effect on reduction, despite both being previously shown to inhibit AKR1C family enzymes (Malátková and Wsól, 2014). This difference could be due to variability in AKR1C inhibition by flufenamic acid depending on the substrate being metabolized, as shown in previous studies (Malátková and Wsól, 2014). Overall, these results suggest that AKR1C family enzymes and CBR1 participate in the reduction of *R*- and *S*-warfarin.

Discussion

Herein, we demonstrated that stereospecificity played an important role in the efficiency of warfarin reduction and the corresponding metabolites generated in the process. This metabolic pathway is low affinity and high capacity, although it is likely underutilized under in vivo conditions. These insights from the kinetics differ from previous reports relying on rac-warfarin and a failure to resolve parent drugs and their metabolites in the analyses. We replicated the findings of others and demonstrated how the experimental design confounds an accurate understanding of *R*- and *S*-warfarin reduction. Our subsequent phenotyping studies revealed the probable cytosolic reductases responsible for stereospecific metabolism of warfarin. Collectively, these findings provide a strong foundation for further studies, such as genotyping of reductases, to explore the clinical relevance of *R*- and *S*-warfarin in patients undergoing anticoagulant therapy.

Our data show that human cytosolic reductases more efficiently metabolized R-warfarin over S-warfarin and preferentially generate S alcohols in the process, which is consistent with previous studies involving both humans and animal models (Lewis, 1974; Hermans and

DMD Fast Forward. Published on June 23, 2017 as DOI: 10.1124/dmd.117.075929
This article has not been copyedited and formatted. The final version may differ from this version.

Thijssen, 1992). According to our kinetics, warfarin reduction is a low affinity but high capacity metabolic pathway that is likely underutilized under in vivo conditions. Maintenance dosing to achieve a targeted therapeutic response results in low micromolar levels of *R*- and *S*-warfarin in plasma (1518 to 4500 nM as compiled in (Haque et al., 2014)). The amounts accessible for reduction are likely about 50-fold lower (mid-nanomolar range) due to high plasma protein binding (O'Reilly, 1986). A possible limitation of this estimation is the lack of consideration of warfarin accumulation in the liver. Studies with rats have shown liver warfarin levels are possibly three-fold higher than that observed in plasma (Levy et al., 2003; Sun et al., 2015). The similarities in physiology between rats and humans suggest that warfarin accumulation in liver is possibly occurring in humans. Even taking this effect into consideration, in vivo levels of *R*- and *S*-warfarin would not approach saturation, so that their reductive elimination would present as essentially linear kinetics in patients.

Steady-state reduction of rac-warfarin by human liver cytosol yielded similar results to that reported by others (Moreland and Hewick, 1975; Alshogran et al., 2015b; Malátková et al., 2016), yet we were able to provide a more in-depth analysis of the data given our kinetics for the individual drug enantiomers. Despite the use of different human liver cytosolic fractions, warfarin alcohol 2 was the major metabolite while warfarin alcohol 1 was the minor one. The V_{max} and K_m values for the alcohol 2 reaction were nearly identical between the studies, as shown in Table 1. The corresponding values for alcohol 1 were within two-fold of one another; that difference could be due to error in the noise in data for the minor pathway. In our case, we can identify likely metabolites contributing to observed kinetic profiles for warfarin alcohols 1 and 2. The RS-warfarin alcohol is the primary contributor to the alcohol 2 and SS-warfarin alcohol to the alcohol 1. SR- and RR-Warfarin alcohols would still contribute to observed mixtures of alcohols as metabolites of the reaction, such that the observed kinetics for rac-warfarin do not represent that for the individual warfarin enantiomers.

DMD Fast Forward. Published on June 23, 2017 as DOI: 10.1124/dmd.117.075929
This article has not been copyedited and formatted. The final version may differ from this version.

Based on the identification of the metabolites, we assessed potential interactions between the warfarin enantiomers that could occur when rac-warfarin served as a substrate. For comparative purposes, we predicted the apparent alcohol 1 and 2 formation rates for rac-warfarin if the R- and S-warfarin did not interact. Under those conditions, observed rates would simply be the summation of the corresponding rates for metabolites contributing to alcohol 1 (*RR*- and *SS*-warfarin alcohols) and alcohol 2 (*RS*- and *SR*-warfarin alcohols) taken from our steady-state data for the reactions with the individual drug enantiomers. As shown in Figure 6, the *predicted* formation rates for warfarin alcohols from rac-warfarin were calculated by summing individual warfarin alcohol rates from warfarin enantiomers as described previously. The *predicted* kinetic profiles significantly differ from the *experimentally* measured values as shown by the dashed lines versus the solid lines. When both drug enantiomers are present, the apparent V_{max} and K_m are lower indicating *R*- and *S*-warfarin interact to impact their reduction to the corresponding alcohols, as has been suggested previously (Chan et al., 1972). Nevertheless, the quantitation of mixtures of the alcohol metabolites precludes the ability to identify the mechanism of interaction and thus understand its impact on major and minor pathways for *R*- and *S*-warfarin reduction. These findings further underscore the complications for relying on rac-warfarin metabolic kinetics to understand its relevance to human metabolism of the drug.

The inhibitor phenotyping indicated that AKR1C3 and CBR1 dominated reductive metabolism of *R*- and *S*-warfarin in the cytosol, while AKR1C1/2 may have made minor contributions. These major enzymes shared similar preference for *R*-warfarin over *S*-warfarin as a substrate and generated *S* alcohols regardless of substrate chirality. This stereospecificity for the cytosolic reductases results in the overall preference formation of the major *RS*-warfarin metabolite followed by the minor *SS*-warfarin metabolite with trace levels of the other warfarin alcohols. Carbonyl reducing enzymes demonstrate stereospecificity that depends on substrate

and the particular enzyme (Hoffmann and Maser, 2007). CBR1 substrates range in molecular mass from 207 g/mol for 4-methylnitrosamino-1-(3-pyridyl)-1-butanone (NNK) to 543 g/mol for doxorubicin (Malatkova et al., 2010), which includes the mass of warfarin (308 g/mol). The enantiospecificity of these reactions has only been reported for NNK in which there is a more than 90% preferential formation of the *S*-alcohol (Breyer-Pfaff et al., 2004), as observed for *R*- and *S*-warfarin reduction in this study. Nevertheless, stereospecificity does vary among individual members of the AKR1C family (Rižner and Penning, 2014).

As further evidence for their role in *R*- and *S*-warfarin metabolism, recombinant AKR1C3 and CBR1 readily catalyzed the reduction of rac-warfarin compared to AKR1B1, 1C1, 1C2, and 1C4 along with CBR3 (Malátková et al., 2016); however, the use of a mixture of *R*- and *S*-warfarin and lack of resolution of substrates and metabolites obscured the stereospecificity of substrate recognition and metabolite formation by the reductases. When considered with respect to our observations, the importance and consequence of AKR1C3 and CBR1 in *R*- and *S*-warfarin becomes more clearly the cause for preferential metabolism of *R*-warfarin and formation of its *RS*-warfarin alcohol metabolite as major reductive pathways in humans.

Concluding Remarks. The kinetics for *R*- and *S*-warfarin metabolism by these reductases could impact clearance of the parent drugs and formation of pharmacologically active metabolites in patients undergoing anticoagulant therapy. For the average patient, *R*-warfarin will primarily undergo reduction compared to *S*-warfarin and thus impact its contributions to anticoagulation (Breckenridge et al., 1974) as well as the resulting less pharmacologically active warfarin alcohol metabolites (Lewis, 1973). The relevance of warfarin reduction on patient dose response variability will depend on genetics, personal habits, and environmental factors that influence reductase activity (Kassner et al., 2008). Xenobiotics including drugs and pollutants interact with aryl hydrocarbon receptor (AhR) to bind to xenobiotic response elements (XRE) that regulate expression and activity of drug metabolizing enzymes including CBR1 (Lakhman et

al., 2007). By contrast, AKR1C are likely regulated through antioxidant regulatory pathways (Burczynski et al., 1999) stimulated by habits suggest as smoking, which induces AKR1C3 levels 15-fold (Nagaraj et al., 2006). That effect could explain why smokers are resistant to warfarin anticoagulation by increasing drug metabolism. Similarly, genetic variants of AKR1C3 (Mindnich and Penning, 2009) and CBR1 (Malatkova et al., 2010) would increase or decrease their roles in warfarin metabolism and hence patient responses, so if shown relevant, the polymorphisms could be incorporated into current pharmacogenetic-based dosing algorithms (Shaw et al., 2015) to improve their predictability. Aside from those unexplored possibilities, the relative contribution of warfarin reduction to the more dominant oxidative pathways remains unknown so that their collective effect on *R*- and *S*-warfarin metabolism requires further investigation. In sum, knowledge of the stereospecificity and efficiency of warfarin reduction provides a critical advance in understanding the overall relevance of metabolism that could impact patient dose-responses.

Authorship Contributions

Participated in Research Design: Barnette, Goodwin, Miller

Conducted Experiments: Barnette, Johnson, Pouncey, Nshimiyimana, Desrochers

Contributed new reagents or analytic tools: Desrochers, Goodwin, Miller

Performed Data Analysis: Barnette, Johnson, Pouncey, Desrochers, Goodwin, Miller

Wrote or contributed to writing of the manuscript: Barnette, Johnson, Pouncey, Goodwin, Miller

References

Alshogran OY, Naud J, Ocque AJ, Leblond FA, Pichette V, and Nolin TD (2015a) Effect of Experimental Kidney Disease on the Functional Expression of Hepatic Reductases. *Drug Metab Dispos* **43:**100-106.

Alshogran OY, Urquhart BL, and Nolin TD (2015b) Downregulation of Hepatic Carbonyl Reductase Type 1 in End-Stage Renal Disease. *Drug Metab Lett* **9:**111-118.

Ansell J, Hirsh J, Hylek E, Jacobson A, Crowther M, and Palareti G (2008) Pharmacology and management of the vitamin K antagonists: American College of Chest Physicians Evidence-Based Clinical Practice Guidelines. *Chest* **133:**160S - 198S.

Breckenridge A, Orme M, Wesseling H, Lewis RJ, and Gibbons R (1974) Pharmacokinetics and pharmacodynamics of the enantiomers of warfarin in man. *Clin Pharmacol Ther* **15:**424-430.

Breyer-Pfaff U, Martin H-J, Ernst M, and Maser E (2004) ENANTIOSELECTIVITY OF CARBONYL REDUCTION OF 4-METHYLNITROSAMINO-1-(3-PYRIDYL)-1-BUTANONE BY TISSUE FRACTIONS FROM HUMAN AND RAT AND BY ENZYMES ISOLATED FROM HUMAN LIVER. *Drug Metab Dispos* **32:**915-922.

Burczynski ME, Lin H-K, and Penning TM (1999) Isoform-specific Induction of a Human Aldo-Keto Reductase by Polycyclic Aromatic Hydrocarbons (PAHs), Electrophiles, and Oxidative Stress: Implications for the Alternative Pathway of PAH Activation Catalyzed by Human Dihydrodiol Dehydrogenase. *Cancer Res* **59:**607-614.

Byrns MC and Penning TM (2009) Type 5 17β-hydroxysteroid dehydrogenase/prostaglandin F synthase (AKR1C3): Role in breast cancer and inhibition by non-steroidal anti-inflammatory drug analogs. *Chem Biol Interact* **178:**221-227.

Chan KK, Lewis RJ, and Trager WF (1972) Absolute configurations of the four warfarin alcohols. *J Med Chem* **15:**1265-1270.

Gebauer M (2007) Synthesis and structure-activity relationships of novel warfarin derivatives. *Bioorg Med Chem* **15:**2414-2420.

Haque JA, McDonald MG, Kulman JD, and Rettie AE (2014) A cellular system for quantitation of vitamin K cycle activity: structure-activity effects on vitamin K antagonism by warfarin metabolites. *Blood* **123:**582-589.

Hermans JJ and Thijssen HH (1992) Stereoselective acetonyl side chain reduction of warfarin and analogs. Partial characterization of two cytosolic carbonyl reductases. *Drug Metab Dispos* **20:**268-274.

Hoffmann F and Maser E (2007) Carbonyl Reductases and Pluripotent Hydroxysteroid Dehydrogenases of the Short-chain Dehydrogenase/reductase Superfamily. *Drug Metab Rev* **39:**87-144.

Jones DR, Kim SY, Boysen G, Yun CH, and Miller GP (2010) Contribution of Three CYP3A Isoforms to Metabolism of R- and S-Warfarin. *Drug Metab Lett* **4:**213-219.

Jones DR and Miller GP (2011) Assays and applications in warfarin metabolism: what we know, how we know it and what we need to know. *Expert Opin Drug Metab Toxicol* **7:**857-874.

Kassner N, Huse K, Martin H-J, Gödtel-Armbrust U, Metzger A, Meineke I, Brockmöller J, Klein K, Zanger UM, Maser E, and Wojnowski L (2008) Carbonyl Reductase 1 Is a Predominant Doxorubicin Reductase in the Human Liver. *Drug Metab Dispos* **36:**2113-2120.

Kim H, Yen C, Preston P, and Chin J (2006) Substrate-Directed Stereoselectivity in Vicinal Diamine-Catalyzed Synthesis of Warfarin. *Organic Lett* **8:**5239-5242.

Laffin B and Petrash M (2012) Expression of the Aldo-Ketoreductases AKR1B1 and AKR1B10 in Human Cancers. *Front Pharmacol* **3**. 104.

Lakhman SS, Chen X, Gonzalez-Covarrubias V, Schuetz EG, and Blanco JG (2007) Functional Characterization of the Promoter of Human Carbonyl Reductase 1 (CBR1). Role of XRE Elements

in Mediating the Induction of CBR1 by Ligands of the Aryl Hydrocarbon Receptor. *Mol Pharmacol* **72:**734-743.

Levy G, E. Mager D, Cheung WK, and Jusko WJ (2003) Comparative pharmacokinetics of coumarin anticoagulants L: Physiologic modeling of S-warfarin in rats and pharmacologic target-mediated warfarin disposition in man. *J Pharm Sci* **92:**985-994.

Lewis R, Trager, WF, Chan, KK, Breckenridge, A, Orme, M, Roland, M, Schary, W (1974) Warfarin. Stereochemical aspects of its metabolism and the interaction with phenylbutazone. *J Clin Invest* **53:**1607-1617.

Lewis R, Trager, WF, Robinson, AJ, Chan, KK (1973) Warfarin metabolites: the anticoagulant activity and pharmacology of warfarin alcohols. *J Lab Clin Med* **81:**925-931.

Malatkova P, Maser E, and Wsol V (2010) Human Carbonyl Reductases. *Current Drug Metab* **11:**639-658.

Malátková P, Sokolová S, Chocholoušová Havlíková L, and Wsól V (2016) Carbonyl reduction of warfarin: Identification and characterization of human warfarin reductases. *Biochem Pharmacol* **109:**83-90.

Malátková P and Wsól V (2014) Carbonyl reduction pathways in drug metabolism. *Drug Metab Rev* **46:**96-123.

Mindnich RD and Penning TM (2009) Aldo-keto reductase (AKR) superfamily: Genomics and annotation. *Human Genomics* **3:**362-370.

Moreland TA and Hewick DS (1975) Studies on a ketone reductase in human and rat liver and kidney soluble fraction using warfarin as a substrate. *Biochem Pharmacol* **24:**1953-1957.

Nagaraj NS, Beckers S, Mensah JK, Waigel S, Vigneswaran N, and Zacharias W (2006) Cigarette smoke condensate induces cytochromes P450 and aldo-keto reductases in oral cancer cells. *Toxicol Lett* **165:**182-194.

O'CONNOR T, IRELAND LS, HARRISON DJ, and HAYES JD (1999) Major differences exist in the function and tissue-specific expression of human aflatoxin B1 aldehyde reductase and the principal human aldo-keto reductase AKR1 family members. *Biochem J* **343:**487-504.

O'Reilly R (1986) Warfarin metabolism and drug-drug interactions. , in: *The new dimensions of warfarin prophylaxis: advances in experimental medicine and biology* (Wessler SB, CG Nemerson, Y ed), pp 205-212, Plenum, New York, NY.

Preston Pugh C, Pouncey DL, Hartman JH, Nshimiyimana R, Desrochers LP, Goodwin TE, Boysen G, and Miller GP (2014) Multiple UDP-glucuronosyltransferases in human liver microsomes glucuronidate both R- and S-7-hydroxywarfarin into two metabolites. *Arch Biochem Biophys* **564:**244-253.

Rižner TL and Penning TM (2014) Role of aldo–keto reductase family 1 (AKR1) enzymes in human steroid metabolism. *Steroids* **79:**49-63.

Shaw K, Amstutz U, Kim RB, Lesko LJ, Turgeon J, Michaud V, Hwang S, Ito S, Ross C, Carleton BC, and Group tCCR (2015) Clinical Practice Recommendations on Genetic Testing of CYP2C9 and VKORC1 Variants in Warfarin Therapy. *Ther Drug Monitor* **37:**428-436.

Sun H, Zhang T, Wu Z, and Wu B (2015) Warfarin is an Effective Modifier of Multiple UDP-Glucuronosyltransferase Enzymes: Evaluation of its Potential to Alter the Pharmacokinetics of Zidovudine. *Journal of Pharm Sci* **104:**244-256.

Trager W, Lewis, RJ, Garland, WA (1970) Mass spectral analysis in the identification of human metabolites of warfarin. *J Med Chem* **13:**1196-1204.

Wong TC, Sultana CM, and Vosburg DA (2010) A Green, Enantioselective Synthesis of Warfarin for the Undergraduate Organic Laboratory. *J Chem Educ* **87:**194-195.

Wysowski DK, Nourjah P, and Swartz L (2007) Bleeding complications with warfarin use: a prevalent adverse effect resulting in regulatory action. *Arch Intern Med* **167:**1414-1419.

Zhang L, Zhang H, Zhao Y, Li Z, Chen S, Zhai J, Chen Y, Xie W, Wang Z, Li Q, Zheng X, and Hu X (2013) Inhibitor selectivity between aldo–keto reductase superfamily members AKR1B10 and AKR1B1: Role of Trp112 (Trp111). *FEBS Lett* **587:**3681-3686.

Footnotes

Financial support for undergraduate research was provided in part by the Summer Undergraduate Research Fellowship program sponsored by the Biochemistry and Molecular Biology Department at the University of Arkansas for Medical Sciences (BPJ and DLP), the UAMS Summer Undergraduate Research Program to Increase Diversity in Research under the National Institutes of Health National Heart, Lung and Blood Institute award [R25HL108825] (DLP). In addition, financial support was provided to GPM through a Grant-in-Aid from the SouthWest Affiliate of the American Heart Association [13GRNT16960043] and a pilot study grant provided by the National Institutes of Health [UL1 TR000039] awarded to the University of Arkansas for Medical Sciences along with grants from the National Institutes of Health National Library of Medicine [R01LM012222 and R01LM012482]. The content of this manuscript is solely the responsibility of the authors and does not necessarily represent the official views of the University of Arkansas for Medical Sciences, the American Heart Association, or National Institutes of Health.

TEG gratefully acknowledges funding from the Hendrix College Odyssey and Rwanda Presidential Scholars Programs, as well as from John and Laura Byrd. Funding was provided by the U.S. National Science Foundation for the NMR spectrometer [1040470].

Legends for Figures

Figure 1. Reduction of *R*- and *S*- warfarin introduces a second chiral center to the molecule. The molecular structure of warfarin contains a single chiral center (letter designation in blue italics). The reduction of *R*- and *S*- warfarin introduces a second chiral center to yield a warfarin alcohol so that there are four possible metabolites.

Figure 2. Control experiments to assess optimal conditions for steady state studies. Panel A, impact of buffer on activity. Total warfarin alcohol formation rates over 30 min measured for 500 μM warfarin, 1 mM NADPH and 0.5 mg/mL protein reactions in 50 mM potassium phosphate pH 7.4 (KPi) with or without 5 mM $MgCl_2$ or 50 mM Tris hydrochloride pH 7.4 (Tris-HCl) with or without 5 mM $MgCl_2$. Panel B, impact of co-solvent on activity. Total warfarin alcohol formation rates measured for reactions with 50 μM warfarin, 1 mM NADPH and 0.5 mg/mL protein at 0.5, 1.0, 2.0, or 5.0 % methanol or dimethylsulfoxide (DMSO) co-solvent in 50 mM potassium phosphate pH 7.4. Panel C, impact of protein levels on activity. After 40 min reaction, total warfarin alcohol levels measured for 50 μM warfarin and 1 mM NADPH reactions with 0.25, 0.5 and 1.0 mg protein/mL pooled human liver cytosol in 50 mM potassium phosphate pH 7.4. Panel D, impact of time on activity. Total warfarin alcohol levels measured for reactions of 50 μM warfarin at 10, 20, 40, and 60 min after initiation with NADPH in 50 mM potassium phosphate pH 7.4.

Figure 3. Kinetic profiles for steady-state reduction of *R*- and *S*-warfarin by human liver cytosol. Reduction of *R*- and *S*-warfarin as described in Materials and Methods yielded two alcohols for each set of reactions. Panel A, kinetic profile for *R*-warfarin reduction showing the major (*RS*-warfarin alcohol, dark blue circle) and minor (*RR*-warfarin alcohol, light blue circle) metabolites. Both sets of data were fit to the Michaelis-Menten model and the resulting kinetic constants reported in Table 1. Panel B, expanded view of kinetic profile for *R*-warfarin reduction to *RS*-warfarin alcohol and its corresponding fit of the data. Panel C, kinetic profile for *S*-warfarin

reduction showing the major metabolites (*SS*-warfarin alcohol, dark red circle). *SR*-warfarin alcohol was not quantifiable due to signal at the limit of detection. Data for *SS*-warfarin alcohol were fit to Michaelis-Menten model and resulting kinetic constants reported in Table 1.

Figure 4. Kinetic profile for steady-state reduction of rac-warfarin by human liver cytosol. Reduction of rac-warfarin as described in Materials and Methods yielded unresolved mixtures of metabolites. Panel A, kinetic profile for alcohol 1 (*RR*- and *SS*-warfarin alcohol, light purple circle) and alcohol 2 (*RS*- and *SR*-warfarin alcohols, dark purple circle). Panel B, expanded view of kinetic profile for rac-warfarin reduction to alcohol 1 and its corresponding fit of the data. Both sets of data were fit to the Michaelis-Menten model and the resulting kinetic constants reported in Table 1.

Figure 5. Inhibitor phenotyping of steady state reduction of *R*- and *S*-warfarin by HLC150. Reactions were carried out with two substrate concentrations, 50 μM (Panels A and B) and 500 μM (Panels C and D), 0.25 mg/mL protein, and 1 mM NADPH with inhibitors for specific cytosol reductases at 37 ºC and pH 7.4. Panels A and C depict selective inhibition of *R*-warfarin to *RS*-warfarin alcohol. Panels B and D show selective inhibition of *S*-warfarin to *SS*-warfarin alcohol. Reaction activities were normalized to the average control rate measured for reactions in the absence of inhibition. Rates were reported as percentages of the control rate. The reported activities are averaged from a minimum of five individual experiments ± standard error. Asterisks indicate statistical significance of inhibition compared to control as calculated using Student's t-test (* $p<0.05$, ** $p<0.005$; *** $p < 0.0005$).

Figure 6. Assessment of potential interactions between R- and S-warfarin during metabolism. After *experimentally* determining rac-warfarin kinetics for alcohol 1 and 2 formation (light and dark purple circles, respectively), we *predicted* the apparent alcohol 1 (light purple circles) and 2 (dark purple circles) formation rates by combining our steady-state data for the reactions with the individual drug enantiomers (Figure 3). The *predicted* versus

DMD Fast Forward. Published on June 23, 2017 as DOI: 10.1124/dmd.117.075929
This article has not been copyedited and formatted. The final version may differ from this version.

experimentally measured alcohol 1 and 2 rates were plotted together for comparison. Panel A, *experimentally* determined kinetic profile for rac-warfarin reaction (circles, solid lines) as well as that predicted by metabolism of individual enantiomers (squares, dashed lines). Panel B, expanded view of kinetic profile for rac-warfarin reduction to alcohol 1 and the predicted kinetic profile. Fit of the estimated data to Michaelis-Menten model is shown in dashed line for comparison to that for actual rac-warfarin reactions in solid line.

Tables

Table 1 - Steady state kinetic constants for *R*-, and *S*-, and rac-warfarin reduction by human liver cytosol

Substrate	Metabolite	Best Fit Model[a]	V_{max} (pmol/min/mg protein)	K_m (μM)	Efficiency (V_{max}/K_m)
R-warfarin	*RS*-warfarin alcohol	Michaelis-Menten	155 ± 18	710 ± 160	0.22
	RR-warfarin alcohol	Michaelis-Menten	0.63 ± 0.18	560 ± 330	0.0011
S-warfarin	*SR*-warfarin alcohol	NA[b]	NA[b]	NA[b]	NA[b]
	SS-warfarin alcohol	Michaelis-Menten	41 ± 18	3500[c]	0.012
rac-warfarin	Alcohol 2 (*RS*/*SR*-warfarin alcohols)	Michaelis-Menten	78 ± 10	710 ± 170	0.11
	Alcohol 1 (*RR*/*SS*-warfarin alcohols)	Michaelis-Menten	4.8 ± 0.7	330 ± 130	0.015
rac-warfarin (Malátková et al., 2016)	Alcohol 2 (*RS*/*SR*-warfarin alcohols)	Michaelis-Menten	76.4 ± 6.0	746 ± 93	0.10
	Alcohol 1 (*RR*/*SS*-warfarin alcohols)	Michaelis-Menten	2.0 ± 0.2	248 ± 51	0.0080

[a] Best fit of data was determined between hyperbolic (Michealis-Menten) and non-hyperbolic (Hill equation) models using extra sum-of-squares F-test in GraphPad Prism.

[b] *SR*-Warfarin alcohol was consistently quantifiable only at *S*-warfarin concentrations of 600 μM or greater, yet data could not be reliable fit to any kinetic model.

[c] The predicted K_m was greater than the highest substrate concentration used in this study (1000 μM) due to solubility limits, and thus, there is more error in the kinetic constants than predicted by a fit hence the exclusion of standard error from the Table.

DMD Fast Forward. Published on June 23, 2017 as DOI: 10.1124/dmd.117.075929
This article has not been copyedited and formatted. The final version may differ from this version.

Figures

Figure 1

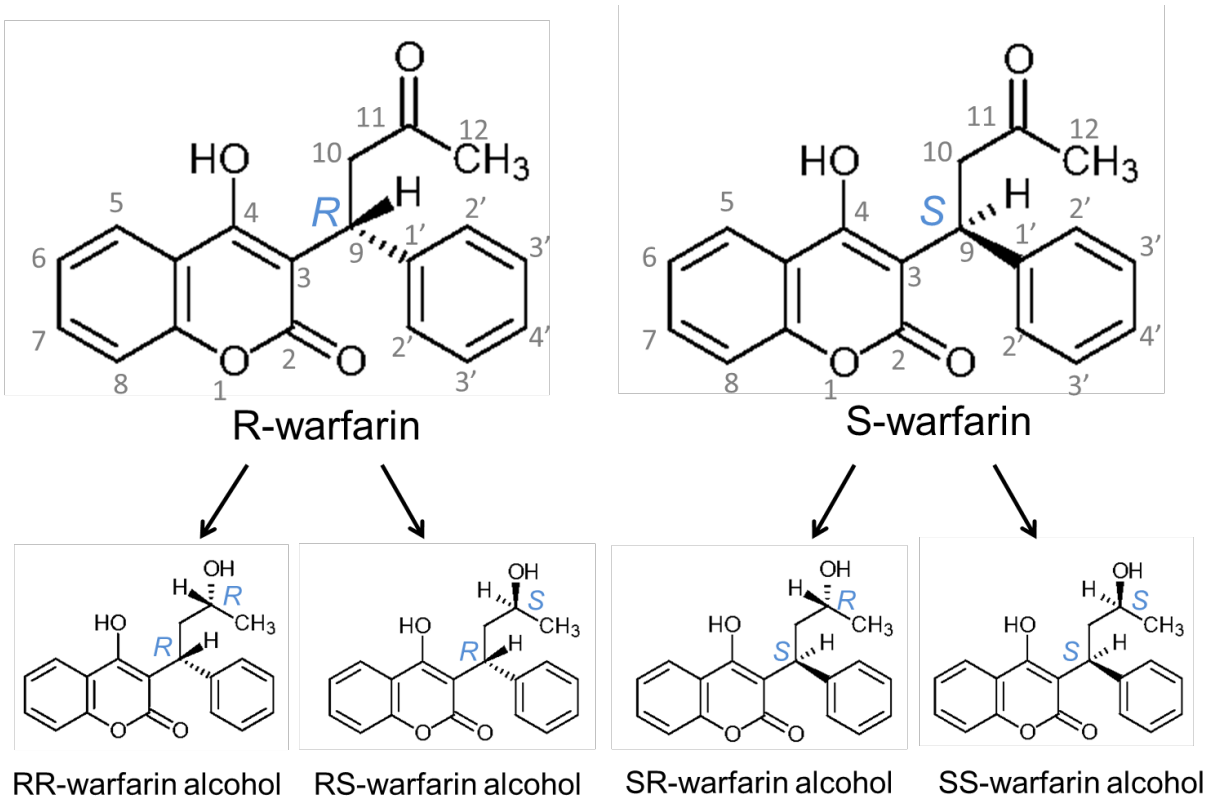

DMD Fast Forward. Published on June 23, 2017 as DOI: 10.1124/dmd.117.075929
This article has not been copyedited and formatted. The final version may differ from this version.

Figure 2

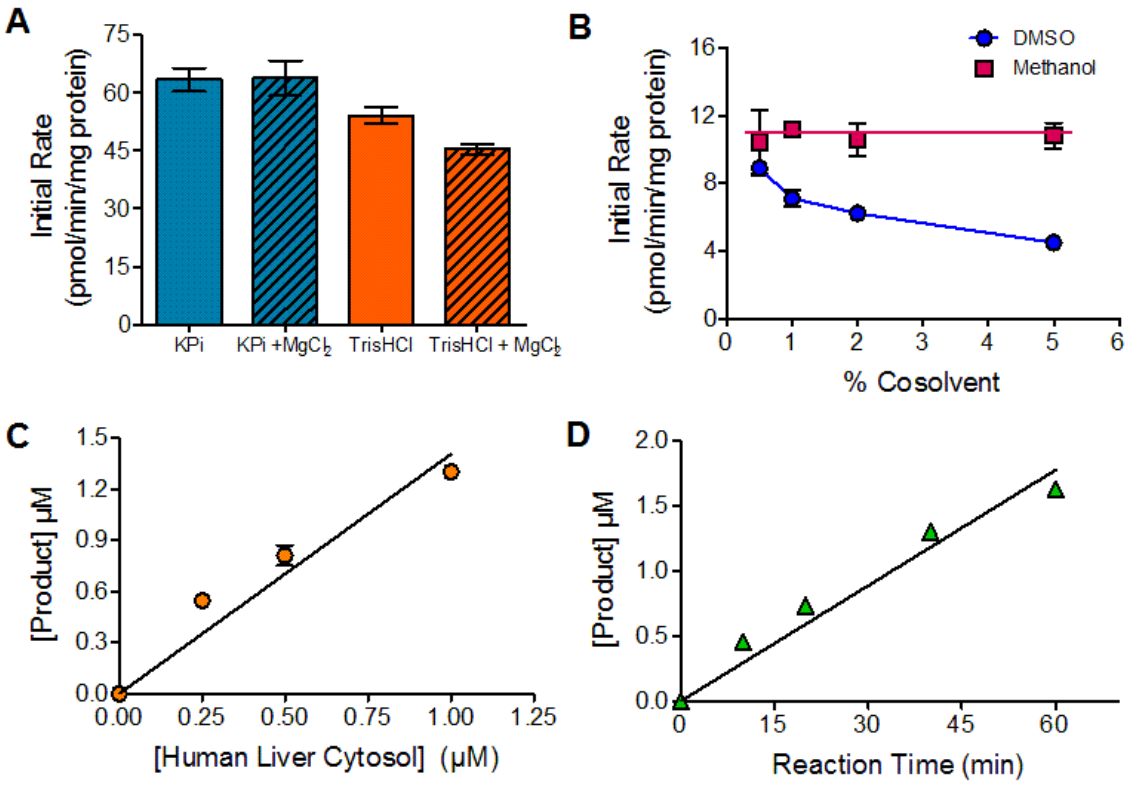

DMD Fast Forward. Published on June 23, 2017 as DOI: 10.1124/dmd.117.075929
This article has not been copyedited and formatted. The final version may differ from this version.

Figure 3

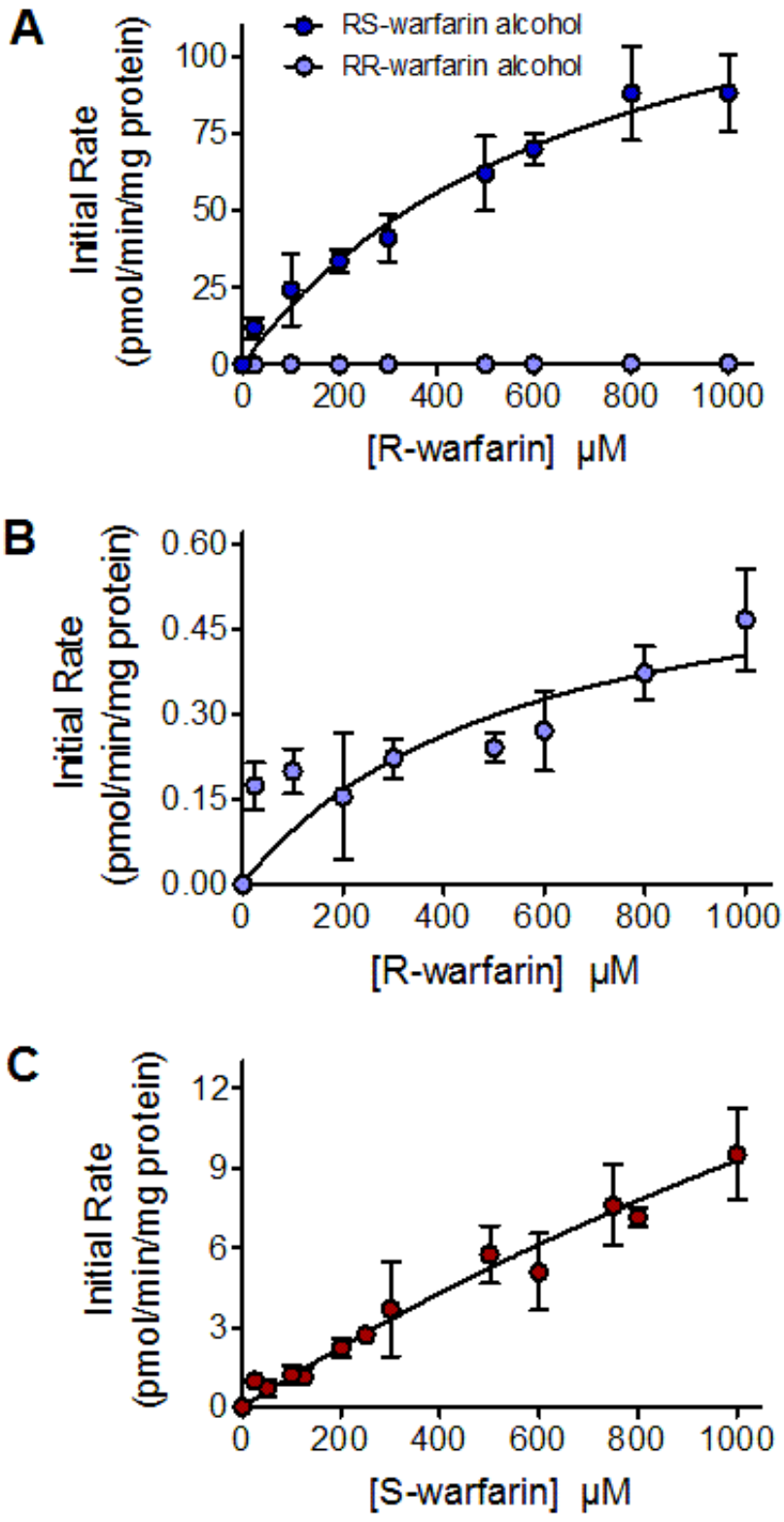

DMD Fast Forward. Published on June 23, 2017 as DOI: 10.1124/dmd.117.075929
This article has not been copyedited and formatted. The final version may differ from this version.

Figure 4

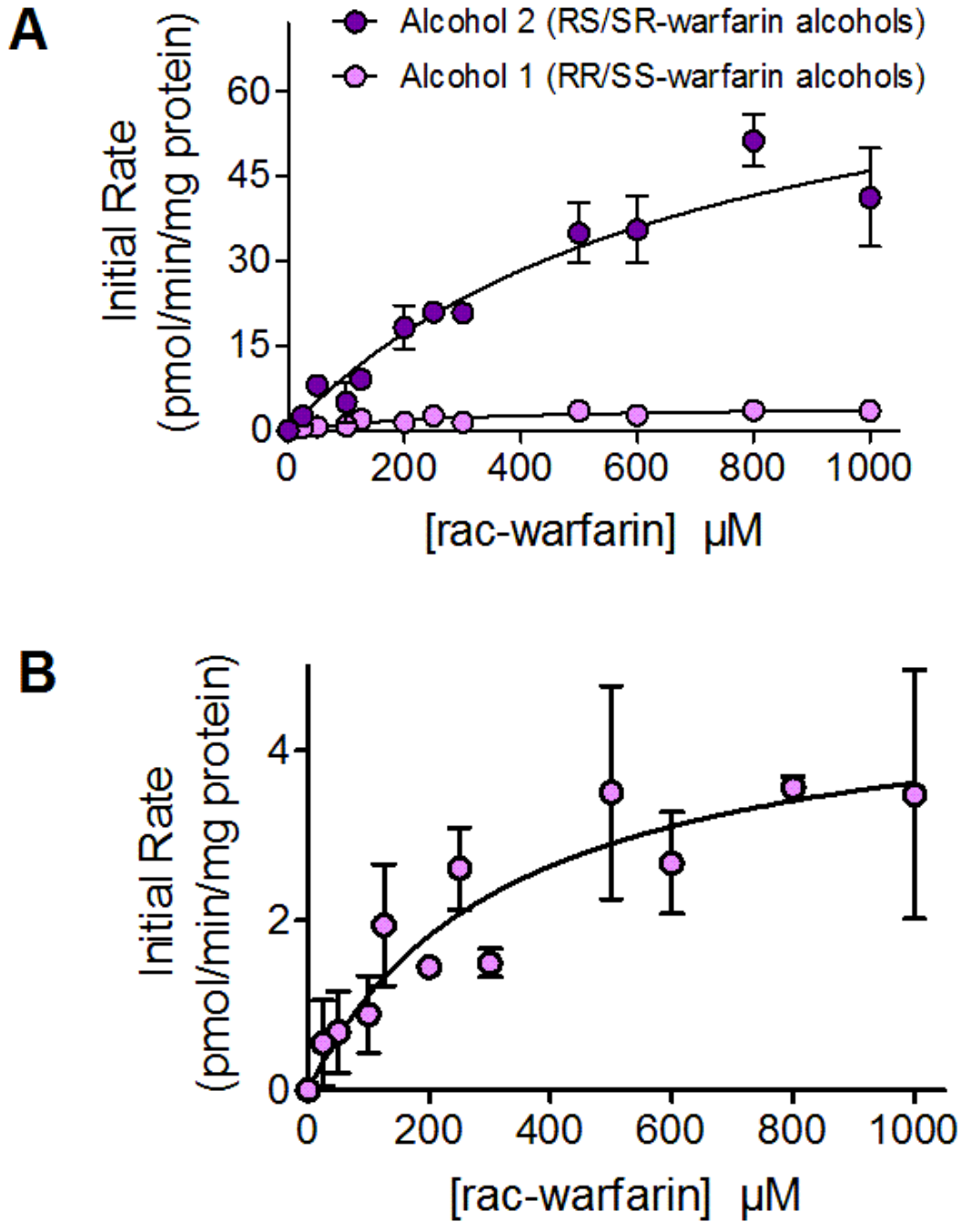

DMD Fast Forward. Published on June 23, 2017 as DOI: 10.1124/dmd.117.075929
This article has not been copyedited and formatted. The final version may differ from this version.

Figure 5

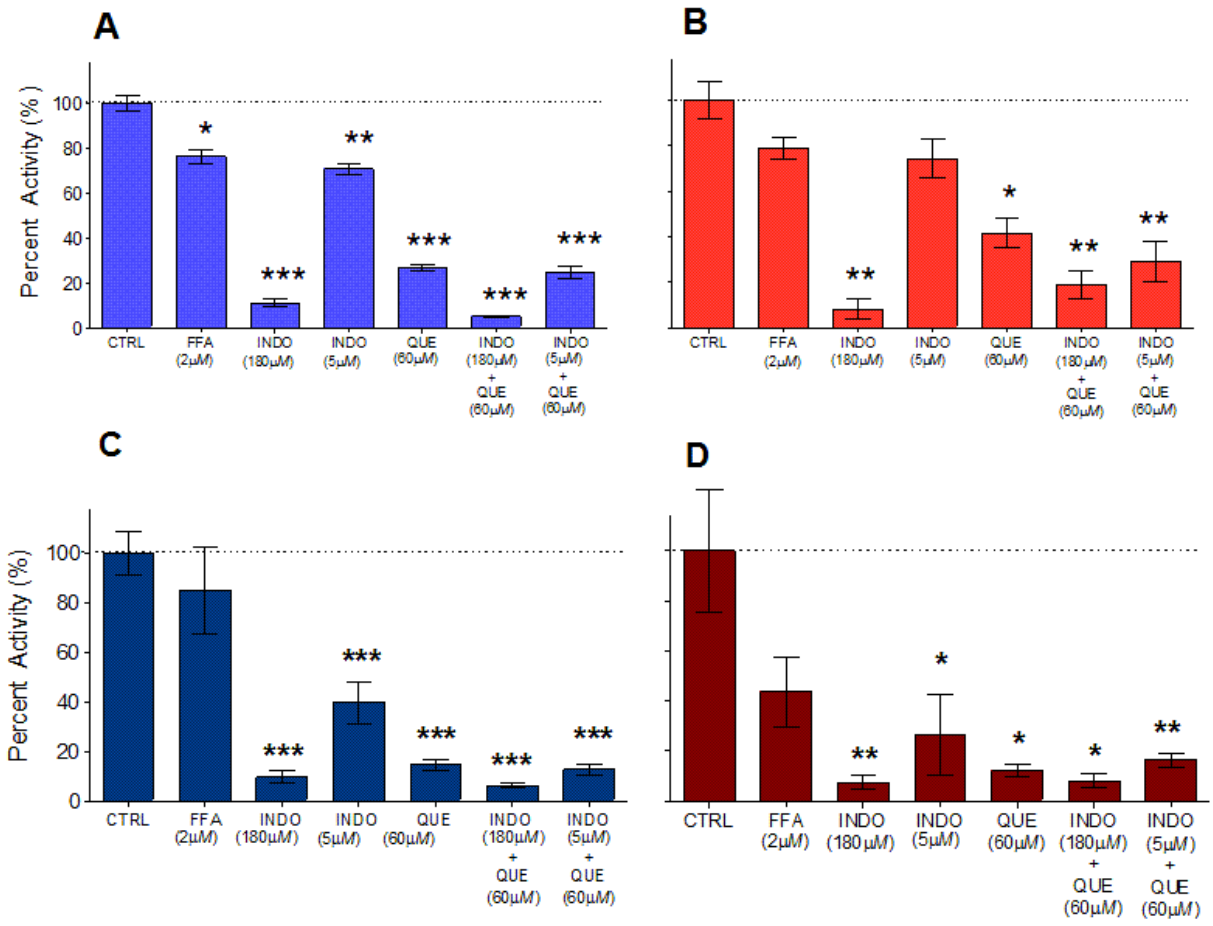

DMD Fast Forward. Published on June 23, 2017 as DOI: 10.1124/dmd.117.075929
This article has not been copyedited and formatted. The final version may differ from this version.

Figure 6